# Induced Capacitance in the Squid Giant Axon

## *Lipophilic Ion Displacement Currents*

JULIO M. FERNÁNDEZ, ROBERT E. TAYLOR, and FRANCISCO BEZANILLA

From the Department of Physiology, Ahmanson Laboratory of Neurobiology and Jerry Lewis Neuromuscular Research Center, University of California, Los Angeles, California 90024; the Marine Biological Laboratory, Woods Hole, Massachusetts 02543; and the Laboratory of Biophysics, National Institutes of Neurological and Communicative Disorders and Stroke, National Institutes of Health, Bethesda, Maryland 20205

ABSTRACT Voltage-clamped squid giant axons, perfused internally and externally with solutions containing $10^{-5}$ M dipicrylamine ($DpA^-$), show very large polarization currents ($\geq 1$ mA/cm$^2$) in response to voltage steps. The induced polarization currents are shown in the frequency domain as a very large voltage- and frequency-dependent capacitance that can be fit by single Debye-type relaxations. In the time domain, the decay phase of the induced currents can be fit by single exponentials. The induced polarization currents can also be observed in the presence of large sodium and potassium currents. The presence of the $DpA^-$ molecules does not affect the resting potential of the axons, but the action potentials appear graded, with a much-reduced rate of rise. The data in the time domain as well as the frequency domain can be explained by a single-barrier model where the $DpA^-$ molecules translocate for an equivalent fraction of the electric field of 0.63, and the forward and backward rate constants are equal at $-15$ mV. When the induced polarization currents described here are added to the total ionic current expression given by Hodgkin and Huxley (1952), numerical solutions of the membrane action potential reproduce qualitatively our experimental data. Numerical solutions of the propagated action potential predict that large changes in the speed of conduction are possible when polarization currents are induced in the axonal membrane. We speculate that either naturally occurring substances or drugs could alter the cable properties of cells in a similar manner.

### INTRODUCTION

Membrane capacitance is an important factor in cellular function. In the case of an axon, for example, it can be shown that the main factors limiting the speed at which depolarization spreads are the axoplasmic resistance and the specific membrane capacitance. The membrane capacitance of cells is impor-

Address reprint requests to Dr. J. M. Fernández, Dept. of Physiology, School of Medicine, Center for the Health Sciences, University of California, Los Angeles, CA 90024.

J. GEN. PHYSIOL. © The Rockefeller University Press. · 0022-1295/83/09/0331/16 $1.00 331

Volume 82 September 1983 331–346

tant in many other processes, such as integration in post-synaptic terminals or dendrites. This paper will demonstrate that the membrane capacitance of the squid giant axon can be modified by addition of hydrophobic ions, which suggests a possible mechanism for the modulation of cell function.

It has been shown (Taylor et al., 1982) that a large fraction of the total capacitance measured in the squid giant axon membrane arises from reorientation of charged or dipolar groups residing in the membrane. This result suggests that variations in these groups from cell to cell or within the same cell would have a large effect on the membrane capacitance and thus on the speed of propagation of action potential or many other cellular functions. Furthermore, any membrane-bound molecule that is charged or has a net dipole moment will make a contribution to membrane capacitance, whether that molecule comes from external sources (drugs, secreted substances), or intrinsic membrane components (sodium channels, membrane-bound enzymes). The characteristics of the resulting capacitance will be a function of the physical properties of the membrane-bound charged molecule.

The feasibility of promoting capacitive changes in a membrane can be demonstrated by the use of hydrophobic ions such as tetraphenylborate or dipicrylamine, which strongly adsorb at the membrane-solution interface and translocate across the membrane under the influence of the transmembrane electric field, producing a net charge movement and consequently contributing to the membrane capacitance.

Charge movement induced by hydrophobic ions has been demonstrated in bilayers (for references, see Szabo, 1977) and also in excitable membranes such as the node of Ranvier (Benz and Nonner, 1981) and the squid giant axon (Benz and Conti, 1981); however, they have been used as probes of membrane structure without exploring their effect on the total membrane capacitance or the excitability of the cell under study.

In this work we study the effect of the hydrophobic ion dipicrylamine ($DpA^-$) on the membrane capacitance and excitability of the squid giant axon. Our results indicate that large changes of the membrane capacitance can be promoted. We also found that the effects of the induced capacitance on the excitable properties of the cell can be qualitatively modeled by modifying the Hodgkin-Huxley (1952) equations so as to include the $DpA^-$ charge movement. The same model predicts large changes on the conduction velocity dependent upon the amount of induced capacitance.

A preliminary report of this work has been presented (Fernández et al., 1982*c*).

## METHODS

### *General*

All our experiments were performed on internally perfused axons of *Loligo pealei* at the Marine Biological Laboratory, Woods Hole, MA.

The axons were perfused in a chamber identical to that described by Bezanilla et al. (1982). The experimental arrangement to voltage clamp the axons is the same as

described by Fernández et al. (1982*a*), allowing for time- and frequency-domain measurements.

Displacement and/or ionic currents were measured in the time domain with the P/4 procedure. Admittance, $Y(\omega)$, was measured with the PRBS (pseudo random binary sequence; see Clausen and Fernández, 1981) technique as described by Fernández et al. (1982*a*). This technique consists of superimposing a small (2 mV peak to peak) PRBS on a test pulse applied to the axon membrane under voltage clamp. Admittance is then calculated by applying Fourier techniques to the measured membrane potential $v(t)$ and current response $i(t)$ (see Fernández et al., 1982*a*, for complete details of this technique).

Membrane action potentials were recorded by stimulating the axons with short ($\approx$50 $\mu$s) pulses through a 100-k$\Omega$ resistor connected to the axial wire. The pulses were generated by a stimulator (S-5; Grass Instrument Co., Quincy, MA) triggered by the computer-controlled data acquisition unit.

The solutions used were: artificial seawater (ASW): 440 mM NaCl, 10 mM $CaCl_2$, 50 mM $MgCl_2$, and 10 mM Tris(hydroxymethyl)aminomethane at pH 7 from Sigma Chemical Co., St. Louis, MO (Trizma-7). Tris-Cl-tetrodotoxin (TTX): 440 mM Trizma-7, 10 mM $CaCl_2$, and 50 mM $MgCl_2$. 200 NMGFG: 100 mM *N*-methylglucamine (NMG) glutamate, 100 mM NMG fluoride, and 10 mM Trizma-7. 400 KF: 400 mM K fluoride and 10 mM Trizma-7. All solutions were adjusted to an osmolality of 960 mosmol/kg by adding sucrose and maintained at pH 7.2. Measurements of the membrane potential have not been corrected for junction potential of the voltage-measuring electrodes. The convention followed is external solution//internal solution.

### *Data Representation*

We follow the same notation as Fernández et al. (1982*a*). The membrane admittance is defined as:

$$Y(\omega, V) = G(\omega, V) + j\omega C(\omega, V),$$

where $j = \sqrt{-1}$, $\omega = 2\pi f$, $f$ is frequency, and $V$ is the membrane voltage. The various representations of capacitance are (*a*) uncorrected capacitance, $C(\omega, V)$; (*b*) membrane capacitance, $C_m(\omega, V)$, obtained after correcting the total admittance for the estimated series resistance, $R_s$ (Fernández et al., 1982*a*); (*c*) nonlinear membrane capacitance, $C_m^n(\omega, V)$, defined as:

$$C_m^n(\omega, V) = C_m(\omega, V) - C_m(\omega, V_s),$$

where $V$ and $V_s$ indicate the membrane potential at which the capacitance was measured. $V_s$ is an extreme membrane potential such that $C_m(\omega, V_s)$ becomes voltage independent.

Displacement currents induced by the lipophilic ion $DpA^-$, as measured with the P/4 procedure, are defined as $I^n(t, V)$, where $V$ is the absolute membrane potential attained by the test pulse. The area under the current trace, $I^n(t, V)$, represents the total amount of charge moved and is defined as $Q_\infty^n(V)$.

### *Curve Fittings*

Single-exponential and single Debye dispersions were fit numerically to the experimental data $I^n(t, V)$ and $C_m^n(\omega, V)$, respectively, by using a nonlinear least-squares algorithm.

## RESULTS

### *Time-Domain Measurements*

We have studied the effect of perfusing squid giant axons internally and externally with solutions containing $10^{-5}$ M dipicrylamine ($DpA^-$). To separate the $DpA^-$ charge movement from the ionic currents, permeant cations were substituted by Tris(hydroxymethyl)aminomethane (Tris) outside and *N*-methylglucamine (NMG) inside.

A typical experiment is shown in Fig. 1*a*, where the records correspond to the current measured with a P/−4 procedure in response to a test pulse of 90 mV, from a holding potential of −70 mV using a subtracting holding potential (SHP) of −140 mV. The traces shown correspond to the current measured at different times after beginning perfusion with the solutions containing $DpA^-$. It is evident from this figure that perfusion with $DpA^-$ induces a current whose value increases with the perfusion time. After an arbitrary amount of $DpA^-$-induced current has been obtained, the perfusion rate was made minimal so that the amount of current did not significantly change with time during the course of the experiment. Under these conditions, the voltage dependence of the currents is demonstrated in Fig. 1*b*. When test pulses are given to different membrane potentials, the current response can be described by fitting a single exponential to the decaying phase. As indicated in Fig. 1*b*, a single exponential fits the decaying phases of the current at all membrane potentials. The single-exponential fits, however, deviate significantly from the experimental traces during the first 100 μs after the onset of the pulse. This corresponds to the rising phase of the displacement current that we believe is related to the series resistance (see Discussion). The voltage dependence of the time constant of the fits is shown in Fig. 3*b*. It is important to notice that the records shown in Fig. 1 correspond to data uncorrected for series resistance.

### *Frequency-Domain Measurements*

The $DpA^-$-induced charge movement shown in Fig. 1*b* can also be demonstrated as a voltage- and frequency-dependent membrane capacitance, $C_m^n(\omega, V)$.

The capacitance is obtained by measuring the admittance, $Y(\omega, V)$, between the voltage-measuring electrodes of a voltage-clamped axon after perfusion with solutions containing $DpA^-$ (see Methods). The admittance was measured during a test pulse to the indicated membrane potential, from a holding potential of −70 mV (see Methods). As shown in Fig. 2*a*, perfusion with $DpA^-$ can increase the capacitance dramatically; a very large voltage- and frequency-dependent capacitance induced by $DpA^-$ is added to the normal capacitance of the axon. As has been previously described, the normal squid axon membrane capacitance is voltage dependent with a maximum change of ~0.15 μF/cm² (Fernández et al., 1982*a*). The induced capacitance is ~30 times bigger in the case shown in Fig. 2, and dwarfs the normal voltage-dependent capacitance, thereby making it unnecessary to correct for it.

To obtain the true membrane capacitance, $C_m(\omega, V)$, we have to correct

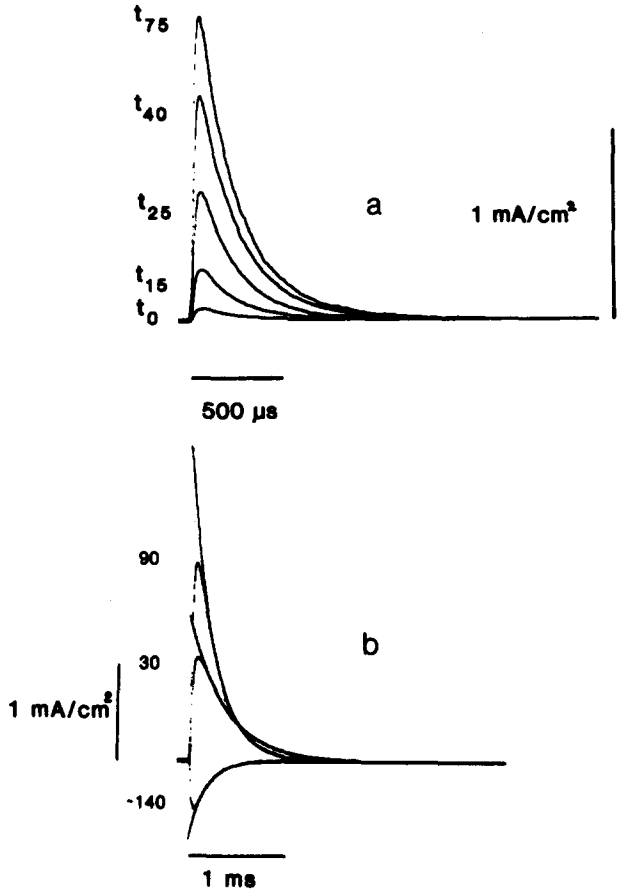


FIGURE 1. Effect of $DpA^-$ on membrane currents in the absence of permeant ions. (*a*) Effect of adding $10^{-5}$ M $DpA^-$ to the internal and external solutions (Tris-Cl-TTX//200 NMGFG). Normal gating currents are shown at time zero. After addition of $DpA^-$, the currents subsequently grow with time as indicated. Currents were measured with the P/4 procedure with a subtracting holding potential (SHP) of −140 mV, pulsing to 20 mV from a holding potential of −70 mV. (*b*) Currents measured with the P/4 procedure, after obtaining a certain amount of $DpA^-$-induced charge movement; perfusion was stopped to minimize the rate of adsorption of $DpA^-$ in the membrane. The currents are voltage dependent and the decay phase can be fit by a single exponential with a voltage-dependent time constant. The single-exponential fits are extrapolated to the onset of the test pulse to indicate the divergence with the rising phase of the recorded currents. The currents were obtained by pulsing to the indicated membrane potential from HP = −70 mV and SHP = −140 mV; Tris-Cl-TTX/ /200 NMGFG.

the admittance, $Y(\omega, V)$, for the estimated series resistance, $R_s$. This correction is done by subtracting $R_s$ from the real part of the total impedance, defined as $Z(\omega, V) = 1/Y(\omega, V)$, and converting back to admittance (Fernández et al., 1982*a*). This procedure is repeated with the admittance data obtained at

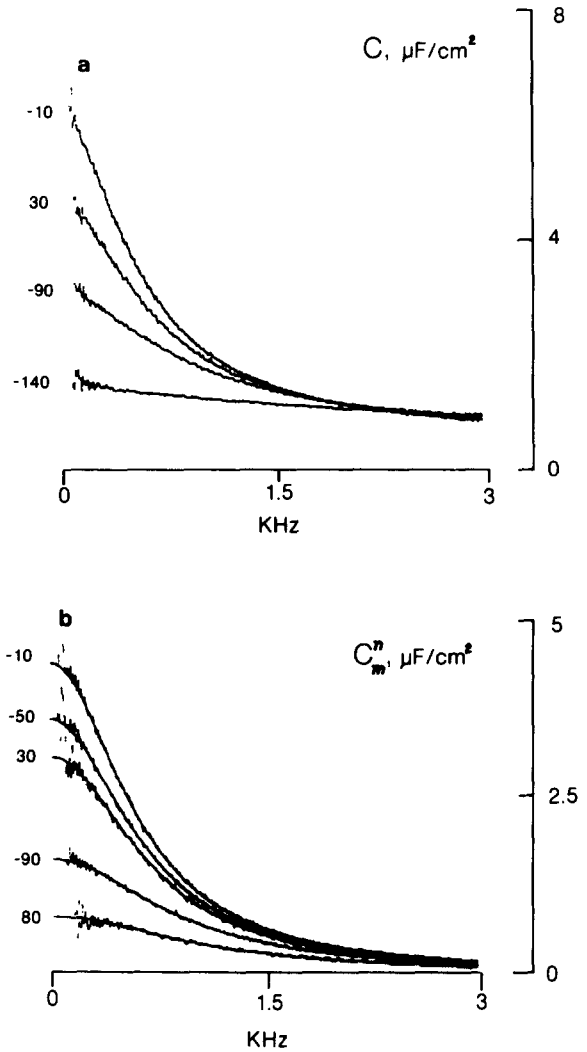


FIGURE 2. Total capacitance measured ~1 h after addition of $10^{-5}$ M $DpA^-$ to the internal and external solutions. (*a*) The resulting capacitance is voltage and frequency dependent and becomes voltage independent for large depolarizations or hyperpolarizations. Capacitance was measured 155 ms after the onset of a test pulse to the indicated membrane potential from a holding potential of −70 mV. Tris-Cl-TTX//200 NMGFG. (*b*) $DpA^-$-induced, voltage-dependent membrane capacitance, obtained after correction for 5 $\Omega cm^2$ of series resistance and subtraction of the voltage-independent capacitance obtained at −140 mV (as shown in *a*). The solid traces correspond to single Debye dispersion fits (see text).

every membrane potential to obtain the membrane capacitance, $C_m(\omega, V)$. The measured value of the total series resistance in our chamber ranged between 4 and 7 $\Omega cm^2$. The value used for correction in Fig. 5*b* was arbitrarily chosen as $R_s = 5\ \Omega cm^2$, which is a reasonable estimate of the actual $R_s$.

To analyze the induced voltage-dependent membrane capacitance, we subtract the voltage-independent capacitance, $C_m(\omega, V_s)$, from the capacitance measured at a different membrane potential, $C_m(\omega, V)$ (see Methods). The voltage-independent capacitance, $C_m(\omega, V_s)$, is measured at very hyperpolarized membrane potentials ($V_s$ less than $-140$ mV). Fig. 2*b* shows the result of applying this procedure to the data of Fig. 2*a*. The resulting voltage-dependent capacitance follows a bell-shaped curve as a function of voltage and has a maximum of 4.5 $\mu F/cm^2$ at about $-15$ mV (see Fig. 3*a*). The induced membrane capacitance, $C_m^n(\omega, V)$, can be simply described by a single Debye dispersion of the form:

$$C_m^n(\omega, V) = \frac{C_0(V)}{1 + \omega^2\tau^2(V)}, \tag{1}$$

where $C_0$ and $\tau$ are voltage-dependent parameters. $C_0$ is the zero-frequency capacitance and $\tau$ is the characteristic time constant or dielectric relaxation time. As shown by the solid traces of Fig. 2*b*, single Debye dispersions fit the data accurately in the whole frequency range. Furthermore, this description of $C_m^n(\omega, V)$ is valid at all membrane potentials.

### *Single-Barrier Model*

Two parameters describe our measurements of $DpA^-$ charge movement in the time domain as well as in the frequency domain: the time constant of the single-exponential fits, $\tau$, and the total amount of charge displaced for any given membrane potential, $Q_\infty^n(V)$, obtained by measuring the area under the current trace. Frequency-domain data give an independent measurement of the relaxation time constant, $\tau(V)$, and the zero-frequency capacitance, $C_0(V)$, both obtained from the single Debye dispersion fits to $C_m^n(\omega, V)$, as shown in Fig. 2*b*. The voltage dependence and magnitude of these parameters is shown in Fig. 3, which corresponds to time- and frequency-domain measurements performed in the same axon. Control measurements showed no change in the amount of $DpA^-$-induced current after perfusion was stopped and during the entire length of the experiment.

Fig. 3*a* shows the voltage dependence of both the charge moved, $Q_\infty^n(V)$, and the zero-frequency capacitance, $C_0(V)$. The solid line corresponds to the predictions of a simple system of $DpA^-$ charges moving between two stable states with a first-order transition. The rate equation for the charge movement, $Q^n(V)$, is:

$$\frac{dQ^n(V)}{dt} = \frac{Q_\infty^n(V) - Q^n(V)}{\tau(V)}, \tag{2}$$

where

$$Q_\infty^n(V) = \frac{Q_T}{1 + \exp\left(\frac{-e\alpha(V - V_0)}{kT}\right)} \tag{3}$$

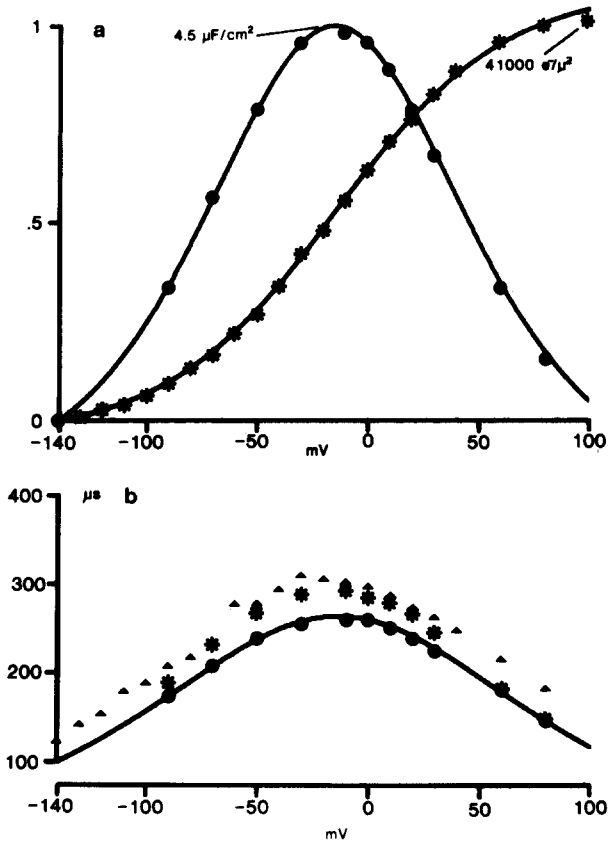


FIGURE 3. $DpA^-$ charge movement parameters as obtained from time- and frequency-domain measurements. (*a*) The stars indicate the total charge moved, $Q_\infty^n(V)$ (see Eq. 3), at the indicated membrane potential, measured by integrating the currents measured in the time domain (see Fig. 1). The filled circles correspond to the zero-frequency capacitance, $C_0(V)$ (see Eq. 5), obtained from the single Debye fits to the voltage-dependent capacitance (see Fig. 2*b*). The solid lines correspond to the predicted voltage dependence of $Q_\infty^n$ and $C_0$ as derived from the single-barrier model with parameters $\alpha = 0.63$ and $V_0 = -15$ mV (see Eqs. 3–6). (*b*) Voltage dependence of the time constant $\tau$. The triangles were obtained from fitting a single exponential to the falling phases of the time-domain currents (e.g., Fig. 1*b*). The stars correspond to the time constant obtained by fitting a single Debye dispersion to the voltage-dependent capacitance without series resistance compensation (fits between 100 Hz and 1 kHz). The filled circles correspond to the time constant obtained by fitting a single Debye dispersion in the whole frequency range, after correction for 5 $\Omega cm^2$ of series resistance (see the data of Fig. 2*b*). The solid line corresponds to the voltage dependence predicted by the single-barrier model used in *a* with identical parameters.

and

$$\tau(V) = \frac{A}{\cosh\left(\frac{e\alpha(V - V_0)}{2kT}\right)}, \tag{4}$$

where $Q_T$ is the total charge available to move, $A$ is equal to the relaxation time constant evaluated at $V = V_0$ (the membrane potential at which half of $Q_T$ is in each stable state), $\alpha$ represents the fraction of the electric distance through which the $DpA^-$ charges translocate, and e, $k$, and $T$ have their usual meanings.

The frequency-domain measurements of the induced membrane capacitance, $C_m^n(\omega, V)$, are predicted when Eq. 2 is linearized around an operation point $p$ (see Taylor and Bezanilla, 1979). This procedure predicts a frequency-dependent capacitance that has the form of a single Debye dispersion:

$$C_m^n(\omega, V) = \frac{C_0(V)}{1 + \omega^2\tau^2(V)}, \tag{5}$$

where the zero-frequency capacitance, $C_0(V)$, is given by:

$$C_0(V) = \frac{Q_T e\alpha/4kT}{\cosh^2\left(\frac{e\alpha(V - V_0)}{2kT}\right)}, \tag{6}$$

and the time constant, $\tau(V)$, is the same as Eq. 4.

The solid lines shown in Fig. 3 correspond to the prediction of the model described above, when $\alpha = 0.63$ and $V_0 = -15$ mV. Fig. 3*b* shows the voltage dependence of the relaxation time constant measured in the time domain (filled triangles) or in the frequency domain, without correcting for series resistance (stars) or after correcting for 5 $\Omega cm^2$. As shown in this figure, the effect of series resistance is to significantly alter the measured value of the time constant as compared with values obtained after correction.

*Effect on Excitability*

We have investigated the effect of the $DpA^-$ charge movement on the normal excitability of the axon. Fig. 4 shows membrane action potentials obtained from an axon perfused with solutions containing normal Na and K concentrations (ASW//400 KFG). The axon had a resting potential of −57 mV. Typical responses for various stimuli are shown. After perfusing the axon for ~1 h with internal and external solutions containing $10^{-5}$ M $DpA^-$, the resting potential was unchanged, but significant changes were observed on the responses to stimuli as shown in Fig. 4*b*. Much larger stimuli were needed to elicit an action potential, and after a stimulus a rapid and large decay preceded any active response, the rate of rise of the action potential was significantly reduced, and the action potentials were more prolonged. These changes are probably due to the induced charge movement. To confirm this, the axon was subsequently voltage clamped, and a charge movement preced-

ing the normal Na and K currents was observed. This can be seen in Fig. 5, where the currents were measured with the P/−4 procedure, applying test pulses to the indicated membrane potential from a holding potential of −70 mV with a subtracting holding potential of −140 mV. In the presence of $DpA^-$, the axons deteriorated faster than normal, and since prolonged exposures were necessary to achieve large displacement currents, somewhat reduced Na and K currents as well as an increased leakage current were

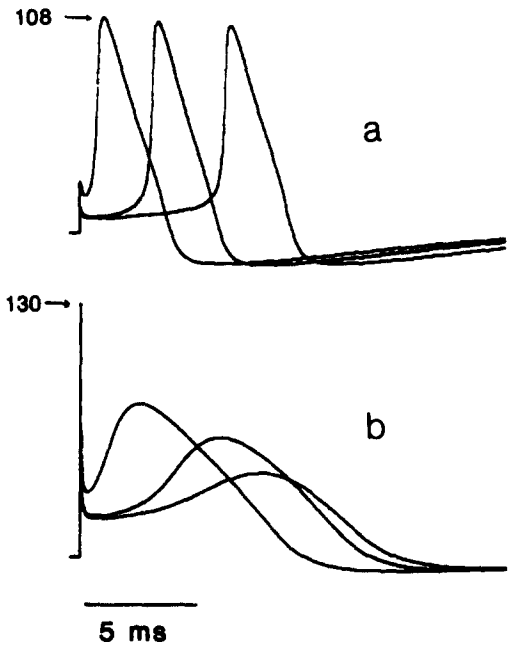


FIGURE 4. Effect of $DpA^-$ charge movement on action potentials. (*a*) Before addition of $DpA^-$, normal membrane action potentials are recorded as shown here for several stimuli; the resting potential was −57 mV and the axon was stimulated with short pulses through a 100-kΩ resistor connected to the axial wire. (*b*) After ~1 h of applying $DpA^-$, the resting potential is unchanged (−57 mV), but much larger stimuli are required to elicit action potentials; a very rapid decay in voltage follows the stimulus and the action potential appears wider with a slower rate of rise. ASW//400 KF.

observed; this may explain the increase in the voltage threshold shown in Fig. 4*b*. Changes in the magnitude, time course, or voltage dependence of the Na and K currents were not studied because the changes, if any, were small compared with the induced charge movement, and also because the incorporation of $DpA^-$ into the membrane is practically irreversible. It is significant that large sodium and potassium currents can be observed in the presence of such large changes of the membrane capacitance.

## DISCUSSION

Our experiments confirm the finding by Benz and Conti (1981) that the lipophilic ion $DpA^-$ is adsorbed into the axolemma and translocates across

the membrane after changes in the membrane electric field.

Voltage-clamp studies of $DpA^-$ charge movement have also been done in the node of Ranvier (Benz and Nonner, 1981); however, it was possible to incorporate only very small amounts of the lipophilic ion into the node membrane (maximum induced currents were only a fraction of normal charge movement), in contrast to the enormous amounts of $DpA^-$ charge movement that can be induced in the squid giant axon membrane. We believe that these results are in good agreement with the hypothesis that lipophilic ions can only be adsorbed in those regions of the membrane that are free from proteins. Since the node has a very high density of channels, very little

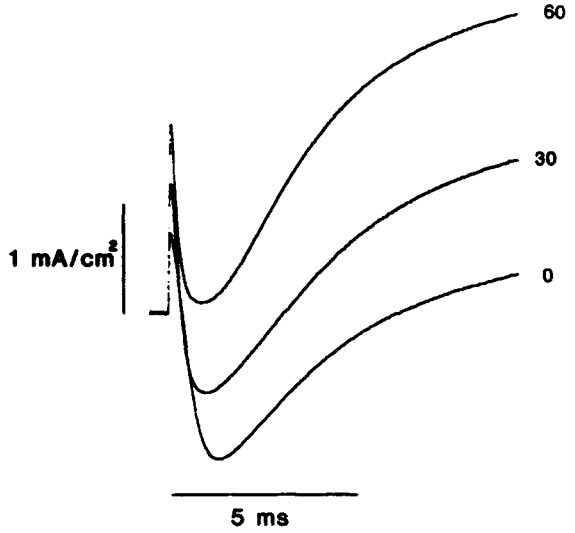


FIGURE 5. Sodium and potassium currents can be observed in the presence of large $DpA^-$-induced charge movement. The currents were measured using a P/−4 procedure with an SHP of −140 mV from an HP of −70 mV and were obtained by voltage clamping an axon after an experiment similar to that shown in Fig. 4*b*. (Fig. 1*b* corresponds to this axon.) ASW//400 KF.

protein-free space remains, whereas the low density of channels in the squid axon membrane would allow much more DpA to be adsorbed.

Because of its simple kinetic behavior and magnitude, the $DpA^-$ charge movement provides ideal experimental conditions to compare time- and frequency-domain methods. As discussed by Fernández et al. (1982*a*), one major advantage of the frequency-domain method is the off-line series resistance correction of the admittance data as compared with the on-line correction necessary in the time domain. The errors introduced by the series resistance are very significant, as shown in Fig. 3*b*, where if no series resistance correction is used, a single-barrier model for $DpA^-$ translocation is inadequate to simultaneously explain $Q_\infty^n$, $C_0$, and $\tau$. Furthermore, when the data are corrected for series resistance, very good fits can be obtained with a single Debye dispersion in the whole frequency range (see Fig. 2*b*). If the data are not corrected, single Debye dispersions fit only in the low-frequency range (100–1,000 Hz), or in the time domain, single exponentials can be fit only

to the latter phase of the response, deviating significantly at short times after the onset of the test pulse (rising phase in Fig. 1*b*). We believe that the corrected data as shown in Figs. 2*b* and 3*b* represent the most accurate determination of the values and voltage dependence of the relaxation time constant.

As shown in Fig. 3*a*, even after pulsing to extreme membrane potentials, saturation of the charge movement is incomplete, making more difficult an accurate determination of parameters such as $V_0$ and $\alpha$. The use of zero-frequency capacitance (which is the slope of the *Q-V* curve) makes the determination of $V_0$ and $\alpha$ much easier, as can be seen in Fig. 3*a*. Furthermore, determinations of $V_0$ do not require measurements at extreme potentials as the time-domain method does since a few potentials around the estimated maximum of $C_m^n$ will give a good estimate of $V_0$. These considerations are useful when lipophilic ions are used to estimate membrane parameters (Benz and Nonner, 1981; Benz and Conti, 1981). Our results agree with those of Benz and Conti (1981) in their observation that $V_0$ is different from 0 mV; we obtain a value of about −15 mV, which is close to the range they suggest.

As shown in Fig. 3, a simple one-barrier model adequately describes the translocation of $DpA^-$ molecules across the axonal membrane. This description, however, is only an approximation, because it does not take into account the rate of adsorption and desorption at the membrane-solution interface or the diffusion rates near the membrane (Szabo, 1977). However, the time constants of these processes are several orders of magnitude larger than the translocation time constant, so the single-barrier model adequately explains the data at short times (e.g., <100 ms) where the influence of adsorption rates is insignificant.

### *Membrane Action Potential*

Hodgkin and Huxley (1952) have formulated a complete mathematical model that adequately describes the generation and propagation of the action potential in the squid giant axon. Their model describes the total membrane current ($I_m$) at any point along the axon, as given by the sum of the capacitative current ($I_c$) and the ionic currents ($I_{ion}$).

The ionic currents have been empirically described by a set of simultaneous differential equations. The capacitative currents were simply considered to be $C_m dV/dt$, where $C_m$ is the specific membrane capacitance (assumed to be 1 $\mu F/cm^2$) and $V$ is the membrane potential. This model does not consider currents caused by dielectric polarization in the membrane.

Adrian (1975) added to the total membrane current ($I_m$) an extra component that accounted for the current contributed by the movement of charges associated with the opening and closing of the sodium channel. We have followed a similar procedure to account for the $DpA^-$ charge movement in the axon membrane.

As shown in Fig. 5, sodium and potassium currents can be observed in the presence of large $DpA^-$ displacement currents. The modeling of the action potential was performed by adding a polarization current produced by $DpA^-$

to the expression of the membrane current presented by Hodgkin and Huxley (1952). In this simulation, we have not considered the lossy part of the membrane capacitance or the polarization currents produced by the charges that gate the sodium and potassium channels.

$$I_m(V) = C_m \frac{dV}{dt} + \frac{dQ^n(V)}{dt} + I_{ion}(V), \tag{7}$$

where $dQ^n(V)/dt$ represents the rate of translocation of the $DpA^-$ charges.

We have solved Eqs. 2–4 and 7 simultaneously with the rest of the Hodgkin-Huxley equations for $V$, assuming that the total membrane current is equal to zero. This corresponds to a space-clamped axon and reproduces the conditions of the experiment shown in Fig. 4. The method of solution was a second-order Runge-Kutta. The parameters used for the calculation of $I_{ion}$ correspond to those used by Hodgkin and Huxley (1952). The parameters used for the calculation of the polarization current, $dQ^n(V)/dt$, are those determined in Fig. 3.

The results of this simulation can be seen in Fig. 6. Fig. 6*a* shows simulated

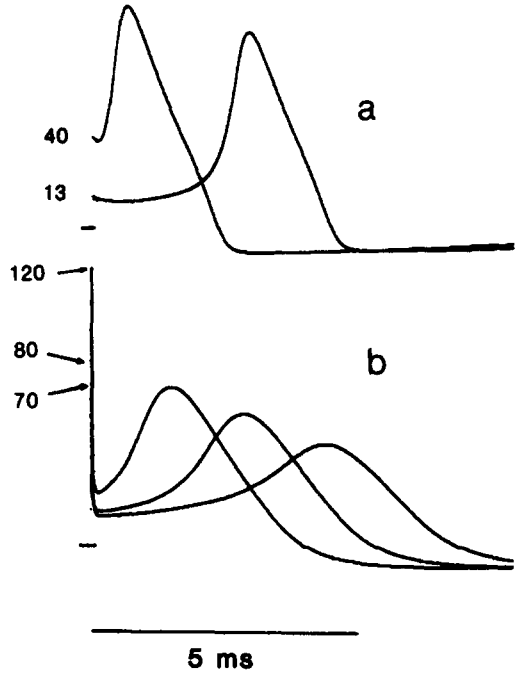


FIGURE 6. Computer simulation of the effect of $DpA^-$ charge movement on the membrane action potential. (*a*) Normal action potential for two stimuli, obtained by solving the H-H differential equations, numerically, using a second-order Runge-Kutta method. (*b*) The effect of adding a total charge movement of 1 $\mu C/cm^2$ can be simulated by adding the charge movement term to the membrane current equation (see Eq. 7). The sodium conductance used in *a* and *b* was 60 $mS/cm^2$, other parameters being identical to those of Hodgkin and Huxley (1952).

action potentials for different stimuli, and assuming no $DpA^-$ charge movement, $dQ^n(V)/dt = 0$. A reduced sodium conductance (60 mS/cm$^2$) is used to simulate real experimental conditions where after prolonged experimentation a reduction in the total sodium currents is inevitable; if the normal (120 mS/cm$^2$) conductance is used, the effect of the extra capacitance on the action potential is qualitatively the same but less pronounced.

When the presence of 1 $\mu$C/cm$^2$ ($Q_T$) of $DpA^-$-induced charge movement is simulated (Fig. 6*b*), the features of Fig. 4*b* can be qualitatively reproduced: after a stimulus, a rapid decay of voltage is followed by an action potential that has a much-decreased rate of rise and is much more spread in time.

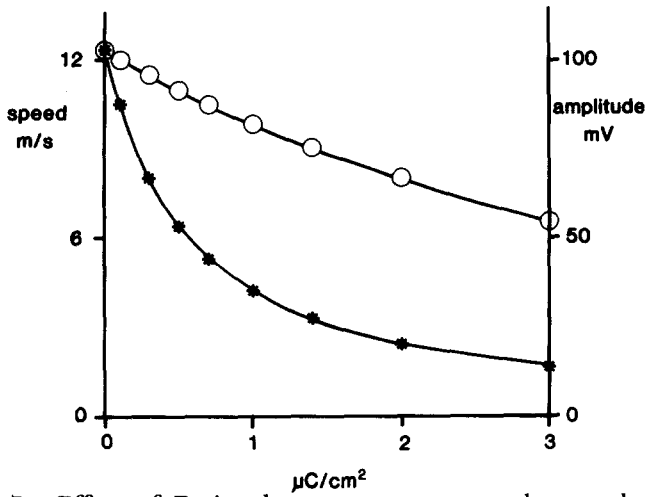


FIGURE 7. Effect of $DpA^-$ charge movement on the speed of conduction (stars) and amplitude (circles) of a propagated action potential obtained by solving Eqs. 2 and 7 and the cable equations for various amounts of $DpA^-$. The solutions were obtained using the Crank-Nicolson implicit method for a cable with 1-mm segments. The simulated axon had a radius of 238 $\mu$m; the temperature was 6.3°C and all other parameters were the same as those of Hodgkin and Huxley (1952). Note that in this case, normal sodium and potassium conductances were used. Velocity was measured after it had reached constant value.

*Conduction Velocity*

We have also investigated the effect of induced charge movement on the speed of conduction of an action potential.

We used an implicit Crank-Nicolson (1947) method of integration to simultaneously solve Eqs. 2 and 7 and the cable differential equations, following the procedure described by Heppner and Plonsey (1970) and Moore et al. (1975). The method is accurate even for large cable segments and calculates the voltage distribution over the whole length of the axon for each time interval.

Computations of the conduction velocity were done assuming an axon with a radius of 238 $\mu$m and a length of 6 cm. The axon was divided into segments;

each segment was 1 mm long and the temperature was 6.3°C. All other parameters of the axon correspond to those used by Hodgkin and Huxley (1952), and the membrane current is given by Eq. 7. Stimulus ranged between 50 and 700 $\mu$A applied for 500 $\mu$s at the initial segment of the axon. The speed of conduction was measured when the action potential reached constant velocity. The results of the simulation are illustrated in Fig. 7, where speed of conduction and amplitude are plotted as a function of the total amount of $DpA^-$ charges available to move ($Q_T$) in the axon membrane. As the results show, large changes in the speed of conduction are possible.

*Significance*

The functional consequences of membrane capacitance are related to neural integration as well as a determinant of the propagation of either active or passive electrical perturbations. The fact that large changes in the membrane capacitance are possible without significant alteration of the normal ionic conductances makes it possible to speculate that exposures of regions of the cell membrane to naturally occurring substances, drugs, or, in diseased cells, by-products of denatured membrane components, could alter the cable-like properties of cells by mechanisms similar to those demonstrated in this paper for the action of $DpA^-$ in the squid axon membrane. Such substances are yet to be found, but their properties should be similar to those of lipophilic ions.

The authors wish to thank Carmen L. Fernández for the careful dissection of all the axons, and Sally Krasne for useful comments.
Supported by a Grass Fellowship to J.M.F. at Woods Hole, an American Heart Association fellowship to J.M.F., and by U.S. Public Health Service grant GM 30376.

*Received for publication 10 January 1983 and in revised form 19 May 1983.*

## REFERENCES

Adrian, R. H. 1975. Conduction velocity and gating current in the squid giant axon. *Proc. R. Soc. Lond. B Biol. Sci.* 189:81–86.

Benz, R., and F. Conti. 1981. Structure of the squid axon membrane as derivated from charge-pulse relaxation studies in the presence of absorbed lipophilic ions. *J. Membr. Biol.* 59:91–104.

Benz, R., and W. Nonner. 1981. Structure of the axolemma of frog myelinated nerve: relaxation experiments with a lipophilic probe ion. *J. Membr. Biol.* 59:127–134.

Bezanilla, F., R. E. Taylor, and J. M. Fernández. 1982. Distribution and kinetics of membrane dielectric polarization. I. Long-term inactivation of gating currents. *J. Gen. Physiol.* 79:21–40.

Clausen, C., and J. M. Fernández. 1981. A low cost method for rapid transfer function measurements with direct application to biological impedance analysis. *Pflügers Arch. Eur. J. Physiol.* 390:290–295.

Crank, J., and P. Nicolson. 1947. A practical method for a numerical evaluation of solutions of partial differential equations of the heat conduction type. *Proc. Cambridge Phil. Soc.* 43:50–67.

Fernández, J. M., F. Bezanilla, and R. E. Taylor. 1982*a*. Distribution and kinetics of membrane dielectric polarization. II. Frequency domain studies of gating currents. *J. Gen. Physiol.* 79:41–67.

Fernández, J. M., F. Bezanilla, and R. E. Taylor. 1982*b*. Effect of chloroform on charge movement in the nerve membrane. *Nature* (*Lond.*). 297:150–152.

Fernández, J. M., R. E. Taylor, and F. Bezanilla. 1982*c*. Gigantic charge movement in the squid giant axon. *Biophys. J.* 37:258*a*. (Abstr.)

Heppner, D. B., and R. Plonsey. 1970. Simulation of electrical interaction of cardiac cells. *Biophys. J.* 10:1057–1075.

Hodgkin, A. L., and A. F. Huxley. 1952. A quantitative description of membrane current and its application to conduction and excitation in nerve. *J. Physiol.* (*Lond.*). 117:500–544.

Moore, J. W., F. Ramon, and R. W. Joyner. 1975. Axon voltage-clamp simulations. I. Methods and tests. *Biophys. J.* 15:11–24.

Szabo, G. 1977. Electrical characteristics of ion transport in lipid bilayer membranes. *Ann. NY Acad. Sci.* 303:266–280.

Taylor, R. E., and F. Bezanilla. 1979. Comments on the measurement of gating currents in the frequency domain. *Biophys. J.* 26:338–340.

Taylor, R. E., J. M. Fernández, and F. Bezanilla. 1982. Squid axon membrane low frequency dielectric properties. *In* The Biophysical Approach to Excitable Systems. Proceedings of Symposium Honoring Kenneth S. Cole on his 80th Birthday. W. J. Adelman and D. E. Goldman, editors. Plenum Press, New York. 97–106.